HHS Public Access

Author manuscript

ACS Infect Dis. Author manuscript; available in PMC 2016 December 13.

Published in final edited form as:

ACS Infect Dis. 2015 June 12; 1(6): 272–283. doi:10.1021/acsinfecdis.5b00036.

Comparative Study of Eis-like Enzymes from Pathogenic and Nonpathogenic Bacteria

Keith D. Green[†], **Rachel E. Pricer**[‡], **Megan N. Stewart**[#], and **Sylvie Garneau-Tsodikova**[*,†]

[†]College of Pharmacy, University of Kentucky, Lexington, Kentucky 40536-0596, United States

[‡]Chemical Biology Doctoral Program, University of Michigan, Ann Arbor, Michigan 48109, United States

[#]Department of Medicinal Chemistry, University of Michigan, Ann Arbor, Michigan 48109, United States

Abstract

Antibiotic resistance is a growing problem worldwide. Of particular importance is the resistance of *Mycobacterium tuberculosis* (*Mtb*) to currently available antibiotics used in the treatment of infected patients. Up-regulation of an aminoglycoside (AG) acetyltransferase, the enhanced intracellular survival (Eis) protein of *Mtb* (Eis_*Mtb*), is responsible for resistance to the second-line injectable drug kanamycin A in a number of *Mtb* clinical isolates. This acetyltransferase is known to modify AGs, not at a single position, as usual for this type of enzyme, but at multiple amine sites. We identified, using in silico techniques, 22 homologues from a wide variety of bacteria, that we then cloned, purified, and biochemically studied. From the selected Eis homologues, 7 showed the ability to modify AGs to various degrees and displayed both similarities and differences when compared to Eis_*Mtb*. In addition, an inhibitor proved to be active against all homologues tested. Our findings show that this family of acetyltransferase enzymes exists in both mycobacteria and non-mycobacteria and in both pathogenic and nonpathogenic species. The bacterial strains described herein should be monitored for rising resistance rates to AGs.

[*]**Corresponding Author**, (S.G.-T.) sylviegtsodikova@uky.edu. Phone: (859) 218-1686. Fax: (859) 257-7585. .

Supporting Information

The following file is available free of charge on the ACS Publications website at DOI: 10.1021/acsinfecdis.5b00036.

9 tables displaying nucleotide and protein sequence numbers for the various Eis homologues studied (Table S1), primers used for cloning (Table S2), and mass analysis for AGs acylated by Eis homologues (Tables S3–S9); 29 figures presenting alignments of Eis homologue protein sequences (Figures S1 and S2), SDS-PAGE gel of purified Eis homologues (Figure S3), representative Michaelis–Menten kinetic plots (Figure S4), and mass spectra of AGs acylated by Eis homologues (Figures S5–S29) (PDF)

The authors declare no competing financial interest.

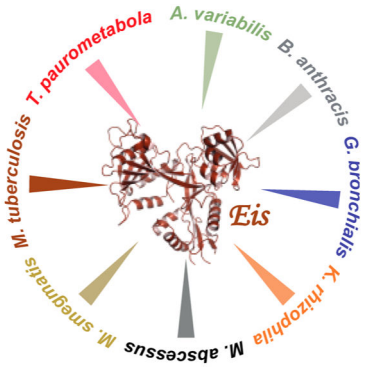

Keywords

acetylation; aminoglycoside acetyltransferases; enzyme inhibitors; n-propionylation; sequential reactions

Resistance to aminoglycosides (AGs, Figure 1) has been a growing problem with numerous species of bacteria, driving the development of novel antibiotics and research into the causes of resistance. Enterococcus faecium, Staphylococcus aureus, Klebsiella pneumoniae, Acinetobacter baumannii, Pseudomonas aeruginosa, and *Enterobacter* species, all together known as the "ESKAPE" pathogens, have been particularly difficult to treat.[1] The most common mode of resistance to AGs is their inactivation by AG-modifying enzymes (AMEs), such as the AG acetyltransferases (AACs), AG phosphotransferases (APHs), and AG nucleotidyltransferases (ANTs). AACs, comprising the majority of these AMEs, are known for their monoacetylating specificities toward the 2′-, 3-, or 6′-positions of a variety of AGs. More recently, a unique AAC, the enhanced intracellular survival (Eis) protein of *Mycobacterium tuberculosis* (*Mtb*), was found capable of multiacetylating AGs.[2,3] It was originally shown that it is the up-regulation of the *eis* gene that is responsible for resistance to kanamycin A (KAN) in a large number of clinical isolates,[4] and since then, numerous additional papers on mutation in the *eis* promoter have been published.[5–7]

We have shown that multiacetylation by Eis completely inactivates AGs.[8,9] We have also performed studies monitoring the effect that different modifications have on a second modification and its catalyzing enzyme.[9] We found that Eis from *Mtb* (Eis_*Mtb*) is capable of multiacetylating AGs,[2] and we observed a similar multiacetylating behavior when studying Eis from *Mycobacterium smegmatis* (Eis_*Msm*1),[10] Eis from *Anabaena variabilis* (Eis_*Ava*),[11] and the Eis homologue from *Bacillus anthracis* (Eis_*Ban*).[37] AACs are known to be cosubstrate promiscuous,[8] although we have shown that Eis_*Mtb* has a much more limited cosubstrate tolerance.[12] In addition, we have studied the metabolically possible competition between acetyl-CoA (AcCoA) and *n*-propionyl-CoA (ProCoA) and the effects it has on multiacetylation of AGs.

Although the cellular role of Eis is still unclear, there have been several proposed functions and substrates for this enzyme. Eis_*Mtb* has been found in the sera of infected patients, suggesting it may play a role in the persistence of bacterial infection.[13] The *eis* protein

product that is secreted from the organism has been proposed to modulate the host inflammatory response.[14] Additionally, T-cells treated with Eis_*Mtb* have an inhibited ERK1/2, JAK pathway, which subsequently produces TNF-α and IL-4, thus disrupting the cross-regulation of T-cells.[15] This effect of aiding the survival of the *Mtb* bacteria in macrophages is thought to be associated with Eis_*Mtb*'s extreme stability under harsh conditions.[16] Suh and co-workers have shown that this modulation of the host immune system may happen through the acetylation of DUSP16/MKP-7 by Eis_*Mtb*[17] and have performed docking studies that corroborate this hypothesis.[18]

In an effort to better understand Eis's role in bacteria and attempt to understand the evolution that occurred with this gene in *Mtb* to modify AGs along with its other substrates, we looked to other bacterial species containing Eis homologues. Through a rigorous in silico search, we found Eis homologues in a variety of mycobacteria and non-mycobacteria (Figure 2). Herein, we examine several properties of these enzymes and compare them to Eis_*Mtb*. We present in silico results for bacterial species containing Eis homologues. We cloned and purified 18 new Eis homologues. We tested these proteins against a small group of antibacterial compounds checking for any acetylation activity. For each AG-active enzyme, we determined the kinetic parameters for a representative of each structural class of AG, kanamycin (KAN) for 4,6-disubstituted deoxystreptamine (DOS) and PAR for 4,5-disubstituted DOS. For combinations producing a positive UV–vis test, we determined the degrees of acetylation and *n*-propionylation. We also explored the cosubstrate tolerance of AG-active enzymes and examined the competition of AcCoA and ProCoA binding in the GNAT domain. In an effort to identify broad or specific inhibitors of these enzymes, a compound known to inhibit Eis_*Mtb*[19] was tested against the AG-active homologues.

RESULTS AND DISCUSSION

In Silico Analysis of Potential Eis Homologues

A BLAST search against Eis_*Mtb* revealed a myriad of Eis homologues. Eis proteins were found in the genome of several mycobacteria including *Mycobacterium avium* subsp. *avium* ATCC 25291 (*Mav*), *Mycobacterium kansasii* ATCC 12478 (*Mka*), *Mycobacterium abscessus* ATCC 19977 (*Mab*), *Mycobacterium hassiacum* DSM 44199 (*Mha*), *Mycobacterium intracellulare* ATCC 13950 (*Min*), and *Mycobacterium parascrofulaceum* ATCC BAA-614 (*Mpa*). Because Eis was originally found in *Mtb*[20] and later in *Msm*,[10] it is not surprising Eis homologues were found in other mycobacteria. Curiously, some species were found to have two (*Mab* and *Mka*) or three (*Mav*, *Min*, and *Mpa*) Eis homologues, and upon further examination of the genomic sequence, a second Eis-like protein was found in *Msm*. Many of the listed mycobacteria are involved in atypical mycobacterial infections,[21] and *Mab* has been noted, particularly, as being "a new antibiotic nightmare";[22] however, this is likely due to mutations in the rRNA,[23] yet drug combinations are being investigated for this pathogenic species.[24] Mav–Min complex, *Mka*, and *M. fortuitum* extracts have been analyzed for AMEs, and an unspecified AAC was found to act on KAN, tobramycin (TOB), and neomycin B (NEO) in *Mka* and *M. fortuitum*.[25] Outside the mycobacterial genus, three other species were found to harbor Eis homologues in their respective genomes: *Gordonia bronchialis* ATCC 25592 (*Gbr*), *Kocuria rhizophila* ATCC 9341 (*Krh*), and *Tsukamurella*

paurometabola ATCC 8368 (*Tpa*). As the name suggests, *Gbr* is a bacterium that often affects the lungs; the sample used here was originally isolated from the sputum of a patient with cavitary pulmonary disease. *Tpa* was originally isolated from the microflora of a bedbug,[26] and *Krh* is a soil microorganism,[27] but is now appearing more often in the clinic.[28,29] A phylogenetic tree (Figure 2) of these proteins was constructed, revealing that these enzymes break into two major groups and three outliers (Eis_*Ava*, Eis_*Ban*, and Eis_*Mab*2). One of the groups consists of strictly proteins from mycobacteria that align well (35% exact amino acid match) with each other and include Eis_*Mab*1, Eis_*Mav*3, Eis_*Mha*, Eis_*Min*2, Eis_*Min*3, Eis_*Mka*2, Eis_*Msm*2, and Eis_*Mpa*3. The second group contains all of the remaining Eis homologues that align poorly (7% exact amino acid match). Taking a closer look at their amino acid sequences, we found most homologues to have the AcCoA binding residues and the catalytic residues in the appropriate position. However, the residues proposed to bind the AG are found to a lesser extent in the homologous enzymes. An amino acid sequence alignment of all 22 Eis homologues is presented in Figure S1 in the Supporting Information, and sequence alignments for AG active and inactive Eis homologues are presented in Figures 3A and S2, respectively.

AG Activity of Eis Enzymes

All Eis homologues were tested against a small library of antibiotic compounds including amikacin (AMK), chloramphenicol (CAM), capreomycin (CAP), ciprofloxacin, hygromycin (HYG), KAN, neamine (NEA), NEO, netilmicin (NET), norfloxacin, paromomycin (PAR), ribostamycin (RIB), sisomicin (SIS), spectinomycin (SPT), and streptomycin (STR) to establish the substrate profile of these enzymes (Table 1). CAM was included in our study because there are known CAM-modifying enzymes;[30] CAP was included because of the recent discovery that Eis_*Mtb* can modify this cyclic peptide;[31] and the fluoroquinolones were included as an AAC mutant was found to acetylate these drugs.[32] Enzymes purified from *Mav*, *Mka*, *Min*, and *Mpa*, along with one enzyme from *Mab* (Eis_*Mab*1) and the new *Msm* enzyme (Eis_*Msm*2), were all found to be AG inactive. These enzymes also all proved to be less soluble than the AG active homologues, with Eis_*Mka*2 being completely insoluble and remaining in the pelleted cell debris under the conditions used to purify Eis_*Mtb*. Eis_*Mha* had excellent expression and solubility, but was also AG inactive under conditions identical to those used in acetylating assays with Eis_*Mtb*. Eis_*Gbr*, Eis_*Krh*, Eis_*Mab*2, and Eis_*Tpa* all showed various degrees of activity with the AGs tested (AMK, HYG, KAN, NEA, NEO, NET, PAR, RIB, and SIS) with the exception of Eis_*Mab*2, which proved to be inactive when tested with AMK. Although the explanation of inactivity of Eis_*Mab*2 toward AMK would be highly speculative without a crystal structure, the 14 Eis homologues showing complete AG inactivity can be analyzed on the basis of their amino acid sequence. Eis_*Mab*1, Eis_*Mav*3, Eis_*Mha*, Eis_*Min*2, Eis_*Min*3, Eis_*Mka*2, Eis_*Msm*2, and Eis_*Mpa*3 all find themselves in one main branch of the phylogenetic tree (Figure 2). It is highly possible that they have some other unknown biological purpose that differs from that of Eis_*Mtb*. One residue that is found to differ from Eis_*Mtb* in all of these AG-inactive Eis homologues is F^{24} (Eis_*Mtb* numbering used throughout). In the majority of these homologues, an arginine residue is found in place of F^{24} (Figure S2). This arginine would repel AGs under physiological conditions. The remaining inactive enzymes are in the second branch of the phylogenetic tree and include the AG-active homologues Eis_*Mtb*,

Eis_*Msm*1, Eis_*Gbr*, Eis_*Krh*, and Eis_*Tpa*. Whereas the homologues from the first branch were missing an important AG binding residue, Eis_*Mav*1, Eis_*Mav*2, Eis_*Min*1, Eis_*Mpa*1, and Eis_*Mpa*2 are all missing one residue for AcCoA binding, R^{128}, which is replaced by either glycine or isoleucine. This lack of charge at this position may not allow AcCoA to bind with affinity similar to that with Eis_*Mtb* (Figure S2). Most surprising is the AG inactivity of Eis_*Mka*1, which has 74% homology to Eis_*Mtb*. The only explanation we can propose from the sequence alignment is that Eis_*Mka*1 is 26 amino acids shorter and is missing amino acid sequences from G^{52} to S^{55}, from L^{158} to S^{161}, and from H^{312} to V^{314}. Upon examination of the Eis_*Mtb* crystal structure (PDB ID 3R1K)[2] these residues form three sites for protein–protein interaction, possibly responsible for oligomerization (Figure 3B) as each missing sequence is in an area where protein–protein interactions are likely to be. This might indicate that Eis_*Mka* does not form hexamers. It has been shown that the Eis_*Mtb* hexameric form is required for activity.[16] It is known that the Eis_*Mtb* hexamer is extremely resilient to a variety of conditions,[16] and based on what we can hypothesize from the Eis_*Mka*1 data, this area could be heavily involved in activity, despite its remote location in relationship to the enzyme active site. Crystal structures of all enzymes would allow for a better understanding of inactivity.

There are structures available for three Eis_*Mtb* homologues, Eis_*Ava*, Eis_*Ban*, and Eis_*Msm*1, which have been previously published with a comparative structural analysis.[2,3,10,11,33,37] Shown in Figure 4 are the four currently known crystal structures of Eis_*Mtb* and its three crystallized homologues. The cartoon overlay of the four crystal structures (Figure 4A) shows only minor changes in the backbone of the structure with only one or two misaligned α-helices and a few disordered loops. The differences are significantly more apparent when looking at the space-filled models (Figure 4B–E), where the AG-binding site (left of the AcCoA-binding site in Figure 4B,D,E) varies. The variance in the AG-binding site is likely why each enzyme reacts with the same AGs differently. Recent work has shown that the AG TOB can bind to Eis_*Mtb* in two distinct orientations, placing two amino groups in the appropriate configuration for acetylation at the 6′- and 3″-positions.[3] This emphasizes the fact that the AG-binding site can dramatically affect not only the identity of AGs that can bind to the Eis enzymes but also the various orientations that any given AG can adopt in the AG-binding pocket.

Acetylation of the Polypeptide Antibiotic CAP

We recently showed that in addition to modifying AGs, Eis_*Mtb* is also capable of acetylating the nonribosomal peptide CAP.[31] In addition to the panel of AGs (Figure 1A), we also tested the seven homologues able to acetylate AGs for their ability to modify CAP. Just as we observed for the AGs, there were several differences within this family of enzymes. Eis_*Krh*, Eis_*Mab*, Eis_*Msm*, Eis_*Mtb*, and Eis_*Tpa* all had very similar initial rates in the UV–vis assay, when CAP was used as the substrate (Figure 5). This suggests that these enzymes all catalyze the modification of CAP similarly. Eis_*Ava* and Eis_*Gbr* both showed significantly reduced reactions rates when modifying CAP, suggesting that these two homologues bind CAP less effectively than the previous five or have a lower catalytic efficiency. Interestingly, Eis_*Ban* did not react with CAP at all. These data supplement the AG data showing that the differences observed in the crystal structures of Eis proteins

(Figure 4) can significantly alter the ability of said enzymes to modify different amino groups.

Kinetic Parameters of AG-Active Eis Homologues for KAN and PAR

Kinetic parameters were determined for Eis_*Gbr*, Eis_*Krh*, Eis_*Mab*2, and Eis_*Tpa* and compared to those previously published for Eis_*Ava*,[11] Eis_*Ban*,[37] Eis_*Msm*1,[10] and Eis_*Mtb*.[2] Kinetic values are presented in Table 2 along with a comparison of the catalytic turnover (k_{cat}) and catalytic efficiency (k_{cat}/K_m) to Eis_*Mtb*. KAN bound with the highest affinity to Eis_*Tpa*, binding 9-fold better than Eis_*Mtb*. Meanwhile, PAR displayed 2.5-fold tighter binding to Eis_*Ban* over Eis_*Mtb*. KAN reacted at a rate of around 0.7 reaction per second with Eis_*Gbr*, 1.28 times faster than Eis_*Mtb*, whereas PAR had the quickest turnover time with Eis_*Tpa* at 5.92 reactions per second, ~44-fold faster than Eis_*Mtb*. The most efficient combinations were with AGs and Eis_*Tpa*, showing ~3- and ~27-fold increases in efficiency for KAN and PAR when compared to Eis_*Mtb*, respectively. Additionally, Eis_*Krh* showed poor kinetic parameters for KAN and heightened parameters for PAR. This is somewhat surprising considering that Eis_*Krh* is roughly 10-kDa larger than Eis_*Mtb*, with two extraneous peptide chains throughout the amino acid sequence (Figure 3A). Although an in-depth kinetic study was not performed for each enzyme, there are no data that indicate that these enzymes do not react similarly to Eis_*Mtb*, having a random sequential mechanism.[34] Whereas Eis_*Mtb* may have evolved to modify AGs due to selective pressure, it seems that the homologues from *Gbr* and *Tpa* have a greater affinity for AGs and these species should be watched for development of AG resistance.

Number of Acetylations

To investigate the extent to which the AG-active Eis homologues can acetylate AGs, we determined the number of sites acetylated by these enzymes on AMK, HYG, KAN, NEA, NEO, NET, PAR, RIB, and SIS (Table 1 and Figures S11, S15, S19, and S26). All Eis homologues were found to acetylate NEA three times. HYG, KAN, and NET all showed mono- or diacetylation by the enzymes, whereas AMK, PAR, RIB, and SIS were observed to be either di- or triacetylated. Interestingly, NEO was acetylated between two and four times. This tetra modification was observed previously only for Eis_*Mtb* and Eis_*Msm*1 with TOB. Only Eis_*Krh*, Eis_*Mab*, and Eis_*Tpa* were found to tetra-acetylate NEO. This suggests that the binding pockets or at least the AG-binding portion of these enzymes are more flexible in their substrate binding. Eis_*Gbr* showed the lowest number of acetylations, in total having monoacetylated three of the AGs tested (HYG, KAN, and NET), suggesting a more limited enzyme–AG interaction. The only other mycobacterial enzyme, Eis_*Mab*, showed similar patterns of acetylation to those of Eis_*Mtb* and Eis_*Msm*1, but was more limited in its substrate profile, not accepting AMK and only diacetylating RIB.

Cosubstrate Tolerance of Eis Enzymes

The AG-active Eis homologues were tested with a variety of acyl-CoAs to establish their cosubstrate promiscuity (Table 3). As we have previously shown, Eis_*Mtb* had a very limited cosubstrate tolerance, transferring acyl groups from AcCoA, ProCoA, crotonyl-CoA, and malonyl-CoA only.[12] In addition to the four acyl-CoAs used by Eis_*Mtb*, *n*-butyryl-CoA, *n*-hexanoyl-CoA, octanoyl-CoA, decanoyl-CoA, lauroyl-CoA, myristoyl-CoA,

palmitoyl-CoA, and *i*-valeryl-CoA were tested as potential cosubstrates. All enzymes could only transfer acyl groups from AcCoA and ProCoA, and Eis_*Krh* could utilize malonyl-CoA to a lesser extent. These data confirm that despite the poor sequence alignment, the CoA-binding pocket of the Eis homologues studied is very likely similar to that of Eis_*Mtb*.

Degree of *n*-Propionylation

The number of *n*-propionylations each enzyme catalyzes with the different AGs was also analyzed to glean more insight into the size of the catalytic pocket (Tables 1 and S3–S9 and Figures S5, S8, S12, S16, S20, S23, and S27). ProCoA, being slightly larger than AcCoA, is not likely to be used as efficiently or result in as many modifications. As expected, all *n*-propionylations were of equal number or less than the number of acetylations observed for the Eis homologue–AG combinations tested. *n*-Propionylation was equal to acetylation for Eis_*Mab*2 in all cases, for seven of nine combinations using Eis_*Ban* (all except KAN and PAR) and Eis_*Gbr* (all except NEA and PAR), six combinations for Eis_*Tpa* (all except AMK, KAN, and NEO), four cases for Eis_*Msm*1 (HYG, KAN, NEO, and NET), and two combinations for Eis_*Ava* (NET and SIS) and Eis_*Krh* (HYG and RIB). These results were equal to or greater than the two cases where *n*-propionylation and acetylation were equal with Eis_*Mtb* (KAN and NEO).[12]

For those combinations that displayed a number of *n*-propionylations lower than that of acetylations, additional experiments were performed to establish if Eis homologues could further acetylate these *n*-propionylated AGs. Sequential acylation reactions in which the enzymes were first allowed to catalyze the *n*-propionylation of the AG for 24 h prior to addition of AcCoA were performed (Tables 4 and S3–S9 and Figures S6, S9, S13, S17, S21, S24, and S28). From these sequential experiments, one could expect to see that (1) no acetyl moiety can be transferred to an *n*-propionylated AG, indicating that *n*-propionylation prevents further acetylation; (2) the total number of modifications (acetylation and *n*-propionylation) equals that of acetylations when only AcCoA is used, indicating that the AG-binding site is likely sufficiently large to accommodate the *n*-propionylated AGs in the same orientation as their corresponding acetylated versions for additional acetylations; or (3) the total number of modifications is less than the number of acetylations observed in the presence of AcCoA alone, likely pointing to the fact that the AG-binding pocket is not large enough to accommodate the extra bulkiness of the *n*-propionyl group on modified AGs in specific orientations in the cavity. In most cases, additional acetylation of *n*-propionylated AGs did occur. The one exception was that of Eis_*Ban*, for which no additional acetylations were observed after *n*-propionylation with the two AGs tested, KAN and PAR. Other combinations where the *n*-propionylation stopped any further modifications included Eis_*Ava* with AMK, NEA, and PAR; Eis_*Krh* with SIS; and finally, Eis_*Msm*1 with NET, RIB, and SIS. Eis_*Mtb* showed limitation with propionylated NET, RIB, and SIS. Although additional acetylations are possible, these results demonstrate that the inability of AGs to become modified with ProCoA as efficiently as AcCoA may lie in the kinetics of the *n*-propionyl transfer rather than the bulkiness of the extra methyl group of the cosubstrate. The remaining results are spread between scenarios 2 and 3. These data indicate that the loss of modification is due primarily to the binding of the modified AG to the enzyme (scenario 3)

or that *n*-propionylation has no effect on acetylation (scenario 2). All observed combinations are presented in Tables 4 and S3–S9.

Cosubstrate Competition of Eis Enzymes

Due to the abundance of both AcCoA and ProCoA in the cellular environment, a competition experiment was performed to gain insight into the kinetic mechanism of the enzymes (Tables 4 and S3–S9 and Figures S7, S10, S14, S18, S22, S25, and S29). AGs were incubated with Eis homologues and a 1:1 mixture of AcCoA and ProCoA and the results analyzed. From these competition experiments, one could expect to observe (1) no *n*-propionylation only acetylation, (2) no acetylation only *n*-propionylation, (3) mixed *n*-propionylation and acetylation, or (4) lower levels of acetylation than incubation with AcCoA alone, due to a competition with the ProCoA for the CoA-binding site. There were no observed cases that follow the second hypothesized observation, meaning that the presence of AcCoA limits the amount of *n*-propionylation that can occur. The most common observation was scenario 3, where there is a majority of acetylation with some *n*-propionylation (usually mono-), followed closely by scenario 4, where less acetylation is observed, likely due to reaction inhibition due to an abundance of CoA-containing molecules. From all these data arise a few interesting cases including NEO with Eis_*Ban*, by which under pure reaction, either AcCoA or ProCoA, only trimodification was observed. When AcCoA and ProCoA are combined, the maximum modification observed is still trimodification (mono-Ac-di-Pro-NEO); however, only diacetyl or dipropionyl-NEO is observed for NEO molecules modified by a single CoA species. Another interesting outcome was the reaction of Eis_*Ban* with PAR; in this reaction we saw monoacetyl-dipropionylated PAR. In the sequential reaction only dipropionylated PAR was observed. These data suggest that acetylation occurred either first or second and *n*-propionylation then occurred. Also of interest is the reaction of Eis_*Gbr* with NEO, after which a whole spectrum of modifications was observed. Everything from triacetyl-NEO to tripropionyl-NEO, including the two possible acetyl-propionyl mixed products, was observed as seen in Tables 4 and S3–S9.

Inhibition of Eis Homologues with Eis_*Mtb* Inhibitors

Knowing that the active sites of the Eis homologues are similar enough to acetylate a variety of AGs and CAP, but different enough to display diverse results, we wondered how these similarities and differences would be reflected in the inhibition of enzymatic activity. Chlorhexidine (Figure 1C), an inhibitor of Eis_*Mtb*,[19] was tested against all seven AG-modifying Eis homologues (Table 5). Although chlorhexidine is used as a topical antibiotic, we used the compound here simply to test if the inhibitor would broadly inhibit all Eis homologues or be specific to Eis_*Mtb* or Eis from mycobacteria. Chlorhexidine displayed a wide range of activities for the Eis homologues, ranging from low nanomolar (Eis_*Mtb*) to micromolar (Eis_*Ava* and Eis_*Ban*). This is an approximate 100-fold range in IC_{50} value, indicating that this inhibitor targets a broad range of Eis homologues. Generally the trend seems to follow that the less homologous the protein is to Eis_*Mtb*, the higher the IC_{50} value, implying a less potent inhibitor. Whereas chlorhexidine would be a poor candidate as an antitubercular drug, it does tell us that inhibitors of Eis_*Mtb* may inhibit other homologues, but an increase in the IC_{50} value could be expected.

In summary, the consolidation of mass spectral analysis, kinetic, inhibitory, and activity data tells us that the Eis homologues share activity, cosubstrate tolerance, and modification multiplicity. We have shown that deletion of 13 residues can render an Eis homologue inactive, and an additional 10 kDa can have a limited effect on activity. Although without structural data these hypotheses are speculative, we have learned that Eis homologues can be found in a diverse community of bacteria and that they behave similarly to Eis_*Mtb*. They also have very distinct sequences, kinetic profiles, and inhibition. Whereas the enzymes do not all come from pathogenic bacteria, the similarity of the enzymes encoded in the genomes of these nonpathogenic species may be a warning that although currently the species do not pose a threat, they may become more aggressive in the future.

METHODS

Phylogenetic Tree Generation

The amino acid sequences of 22 Eis homologues were obtained from NCBI through the Geneious Pro 4.8.5 program to construct a phylogenetic tree (Figure 2). The parameters used were as follows: Jukes–Cantor genetic distance and cost matrix Blosum45. The Eis homologue accession numbers from NCBI were YP_325469 (*Ava*), YP_029001 (*Ban*), YP_003272441 (*Gbr*), YP_001855041 (*Krh*), YP_00170485 (*Mab*1), YP_001705255 (*Mab*2), ZP_05216001 (*Mav*1), ZP_05217647 (*Mav*2), ZP_05214704 (*Mav*3), EKF23162 (*Mha*), ZP_05228133 (*Min*1), ZP_05227568 (*Min*2), YP_005335697 (*Min*3), ZP_04749484 (*Mka*1), ZP_04747464 (*Mka*2), ZP_06852004 (*Mpa*1), ZP_06848356 (*Mpa*2), ZP_06849426 (*Mpa*3), YP_887817 (*Msm*1), YP_888812 (*Msm*2), AAF03768.1 (*Mtb*), and YP_003645809 (*Tpa*). The percent identity of these homolgues to Eis_*Mtb* is presented in Table S1.

Materials and Instrumentation

Chemically competent *Escherichia coli* (TOP10 and BL21 (DE3)) cells were purchased from Invitrogen (Carlsbad, CA, USA). Genomic DNA (*Krh* and *Tpa*) and bacterial strains (*Gbr*, *Mab*, *Mav*, *Min*, *Mka*, and *Mpa*) were purchased from American Type Culture Collection (ATCC; Manassas, VA, USA). Genomic DNA for *Mha*[35] was a gift from Dr. Nuno Empadinhas (University of Coimbra, Portugal). The pET28a plasmid used in this study was obtained from Novagen (Gibbstown, NJ, USA). All primers used were obtained from Integrated DNA Technologies (Coraville, IA, USA). All cloning enzymes including restriction enzymes, Phusion DNA polymerase, and T4 DNA ligase were purchased from New England Biolabs (Ipswich, MA, USA). Sequencing of generated plasmids was performed at the University of Michigan DNA sequencing core. AMK, CAM, CAP, CIP, KAN, NEO, NOR, RIB, SIS, SPT, STR, AcCoA, acyl-CoAs (ProCoA, *n*-butyryl-CoA, *n*-hexanoyl-CoA, octanoyl-CoA, decanoyl-CoA, lauroyl-CoA, myristoyl-CoA, palmitoyl-CoA, crotonyl-CoA, malonyl-CoA, and *i*-valeryl-CoA), and dithionitrobenzoic acid (DTNB) were purchased from Sigma-Aldrich (Milwaukee, WI, USA) and used without further purification. NEA, NET, and PAR were purchased from AK Scientific (Mountain View, CA, USA). All UV–vis assays and kinetic experiments were performed using a multimode SpectraMax M5 plate reader in 96-well plates from Fisher Scientific (Pittsburgh, PA, USA). Liquid chromatography–mass spectrometry (LC-MS) chromatograms were obtained on a

Shimazdu LC-MS-2019EV equipped with an SPD-20AV UV–vis detector and an LC-20AD liquid chromatograph. The PDB structures 2OZG (Eis_*Ava*),[11] 3N7Z (Eis_*Ban*),[37] 3SXN (Eis_*Msm*1),[17] and 3R1K (Eis_*Mtb*)[2] were visualized using PyMOL (The PyMOL Molecular Graphics System, version 1.4.1, Schrödinger, LLC).

DNA Isolation from Bacteria

DNA was isolated from the following bacteria: *M. abscessus* ATCC 19977, *M. kansasii* ATCC 12478, *M. parascrofulaceum* ATCC BAA-614, *M. intracellulare* ATCC 13950, *M. avium* ATCC 25291, and *G. bronchialis* ATCC 25592. Mycobacteria were grown in 7H9 medium with albumin–dextrose–catalase (ADC). One milliliter of turbid culture was pelleted (13000 rpm, 1 min, room temperature) and resuspended in TE buffer (400 μL). The bacteria were inactivated with heat (30 min, 80 °C). After cooling to room temperature, to avoid clumping of the cells, four to five glass beads were added and the cells were briefly vortexed. Lysozyme (30 μL, 50 mg/mL) was added, and the suspension was further incubated for 1 h at 37 °C. At this point SDS (10 μL, 10%) and proteinase K (10 μL, 20 mg/mL) were added, and the suspension was gently vortexed, followed by a brief incubation period (15 min, 65 °C). NaCl (100 μL, 5 M) and CTAB/NaCl (100 μL, 10% CTAB in 0.7 M NaCl) were added sequentially, and the suspension was further incubated (10 min, 65 °C). The mixture was extracted with phenol/chloroform/isoamyl alcohol 25:24:1 (3 × 750 μL). The DNA was precipitated using isopropanol (0.6× volume) and incubated (20 min, −20 °C). The DNA was collected by centrifugation (12000 rpm, 10 min, room temperature), the isopropanol was removed, and the DNA pellet was washed with ice-cold ethanol (75%, 1 mL) and centrifuged (12000 rpm, 5 min, room temperature). The ethanol was removed and allowed to air-dry (10 min, room temperature). The DNA was redissolved in TE buffer (100 μL, 30 min, 37 °C). *G. bronchialis* was grown in BHI, and DNA was isolated as above.

Cloning, Expression, and Purification of Eis Proteins

Eis_*Mtb*,[2] Eis_*Msm*1,[10] Eis_*Ban*,[37] and Eis_*Ava*[11] were cloned and purified as previously described. The remaining Eis proteins were cloned using the isolated DNA, the corresponding primers reported in Table S2, and Phusion DNA polymerase. The isolated PCR fragments were inserted into a linearized pET28a vector between the *Nde*I (all genes) and XhoI (Eis_*Gbr*, Eis_*Krh*, Eis_*Mab*1, Eis_*Mab*2, Eis_*Mha*, and Eis_*Tpa*) or *Hin*dIII (Eis_*Mav*1, Eis_*Mav*2, Eis_*Mav*3, Eis_*Min*1, Eis_*Min*2–3, Eis_*Mka*, Eis_*Mpa*, and Eis_*Msm*2) restriction sites. The plasmids containing the *eis* genes were then transformed into *E. coli* TOP10 chemically competent cells. Sequencing of the isolated plasmid revealed perfect alignment with the reported gene sequences (Table S1). Plasmids were transformed into *E. coli* BL21 (DE3) chemically competent cells for protein expression. All new Eis enzymes were purified exactly as indicated for Eis_*Mtb*.[2] All proteins were dialyzed in Tris-HCl buffer (50 mM, pH 8.0 adjusted at room temperature) and stored at 4 °C. After purification, 2.2 mg (Eis_*Gbr*), 1.8 mg (Eis_*Krh*), 0.1 mg (Eis_*Mab*1), 0.4 mg (Eis_*Mab*2), 3.8 mg (Eis_*Mav*1), 0.8 mg (Eis_*Mav*2), 0.5 mg (Eis_*Mav*3), 7.0 mg (Eis_*Mha*), 2.6 mg (Eis_*Min*1), 1.2 mg (Eis_*Min*2/3), 1.0 mg (Eis_*Mka*1), 0 mg (Eis_*Mka*2, insoluble), 0.4 mg (Eis_*Mpa*1), 0.5 mg (Eis_*Mpa*2), 0.3 mg (Eis_*Mpa*3), 0.5 mg (Eis_*Msm*2), and 1.9 mg (Eis_*Tpa*) of protein were obtained per liter of culture. SDS-PAGE gels showing all Eis homologue proteins purified are presented in Figure S3.

Spectrophotometric Measurements of Acyltransferase Activity

The acyltransferase activity of Eis enzymes was tested against a variety of antibiotics using AcCoA, by monitoring the 2-nitro-5-thiobenzoate (NTB^-) produced by the reaction of free CoA with DTNB. Reactions were monitored at 412 nm ($\varepsilon_{412\ nm}$ = 14150 M^{-1} cm^{-1}) for 1 h, taking measurements every 30 s at 25 °C. Reaction mixtures (200 μL) containing antibiotic (100 μM), AcCoA (500 μM), DTNB (2 mM), and Tris-HCl buffer (50 mM, pH 8.0 adjusted at room temperature) were initiated by the addition of Eis enzyme (0.5 μM). The only non-AG to be modified by Eis enzymes was CAP (Figure 1B); UV–vis curves for this antibiotic are presented in Figure 5. All enzymes displaying activity against AGs were also tested for cosubstrate promiscuity (Table 3). Here acyl-CoAs (ProCoA, *n*-butyryl-CoA, *n*-hexanoyl-CoA, octanoyl-CoA, decaonyl-CoA, lauroyl-CoA, myristoyl-CoA, palmitoyl-CoA, crotonyl-CoA, malonyl-CoA, and *i*-valeryl-CoA) (500 μM) were tested against NEO (100 μM), the most dynamic AG with all AG-active enzymes.

Determination of Number of Acetylations and *n*-Propionylations as well as Sequential and Competitive Modifications of AGs by Eis Proteins via LC-MS

The extent of acetylation for each AG that was found to be active by UV–vis assays (Figure 1A) was determined by using LC-MS. Reactions (30 μL) containing AG (AMK, HYG, KAN, NEA, NEO, NET, PAR, RIB, and SIS, 0.67 mM), AcCoA (3.35 mM), Eis enzyme (5 μM), and Tris-HCl buffer (50 mM, pH 8.0 adjusted at room temperature) were incubated overnight at room temperature. Reactions were quenched by the addition of ice-cold methanol (30 μL) and were chilled (−20 °C) for at least 20 min. To remove excess enzyme from the solution, the reactions were then centrifuged (13000 rpm, 10 min, room temperature) and diluted 1:1 with H_2O before loading onto the LC-MS. Samples were run using H_2O (0.1% formic acid). A summary of the level of acetylation is presented in Table 1. The *n*-propionylation of AGs (AMK, HYG, KAN, NEA, NEO, NET, PAR, RIB, and SIS) was also monitored using the above method substituting ProCoA for AcCoA. A summary of *n*-propionylation is also presented in Table 1. Sequential acylations (*n*-propionylation followed by acetylation) were performed and monitored as above. After the first overnight incubation with ProCoA, AcCoA (3.35 mM) and additional Eis enzyme (5 μM) were added, bringing the total volume up to 40 μL, and incubated for an additional 24 h. A summary of the acylated AG species obtained during sequential experiments is presented in Table 4. Competition experiments were also performed as above in the simultaneous presence of both AcCoA (3.35 mM) and ProCoA (3.35 mM). A summary of the acylated AG species obtained during competition experiments is also presented in Table 4. Calculated and observed masses for all AGs against all Eis homologue proteins are presented in Tables S3–S9, with each table summarizing findings for a specific Eis homologue. Mass spectra for all of these experiments are presented in Figures S5–S29 for Eis_*Ava*, Eis_*Ban*, Eis_*Gbr*, Eis_*Krh*, Eis_*Mab*2, Eis_*Msm*1, and Eis_*Tpa* in the following order: (i) acetylation, (ii) *n*-propionylation, (iii) sequential *n*-propionylation followed by acetylation, and (iv) competition between *n*-propionylation and acetylation.

Determination of Steady-State Kinetic Parameters of Eis Proteins for AGs

The kinetic parameters (k_{cat} and K_m) were determined for acetylation with KAN and PAR for all enzymes, in reactions (200 μL) with a fixed AcCoA (0.5 μM) concentration. For Eis_*Krh*, Eis_*Mab2*, and Eis_*Tpa*, concentrations of 0, 20, 50, 100, 250, 500, 1000, and 2000 μM were used with both AGs. With Eis_*Gbr* the ranges varied, KAN concentrations were 0, 20, 50, 250, 500, and 1000 μM, and PAR concentrations were 0, 20, 50, 100, 250, 500, 1000, and 2000 μM. The reaction cocktail containing DTNB (2 mM), Tris-HCl buffer (50 mM, pH 8.0 adjusted at room temperature), AcCoA (0.5 μM), and Eis enzyme (0.25 μM) was initiated by the addition of the AGs. The reactions were monitored at 412 nm by taking readings every 20 s for 20 min at 25 °C. The determination of kinetic parameters was done with a nonlinear regression using Sigma-Plot 11.0 software (Systat Software Inc., San Jose, CA, USA) (Table 2 and Figure S4).

Inhibition of Eis Enzymes

IC_{50} values for chlorhexidine (Figure 1C) were determined as previously reported.[10,11,19] Briefly, reactions (200 μL) were initiated in a stepwise manner. Chlorhexidine (100 μL) was dissolved in Tris-HCl buffer (50 mM, pH 8.0, 10% DMSO) and subjected to a 5-fold serial dilution. To the chlorhexidine solution was added a mixture (50 μL) of Tris-HCl buffer (50 mM, pH 8.0), Eis enzyme (2 μM), and NEO (400 μM) followed by incubation (10 min, room temperature). A third reaction mixture consisting of Tris-HCl buffer (50 μM, pH 8.0), AcCoA (2 mM), and DTNB (8 mM) was used to initiate the reactions. The reactions were monitored as described for the kinetic analysis. The determination of IC_{50} values was done with a Hill plot analysis using Kaleidagraph 4.1 software, and the data are summarized in Table 5.

Supplementary Material

Refer to Web version on PubMed Central for supplementary material.

ACKNOWLEDGMENTS

This work was supported by NIH Grant AI090048 (to S.G.-T.) and by startup funds from the College of Pharmacy at the University of Kentucky (to S.G.-T.).

REFERENCES

(1). Boucher HW, Talbot GH, Bradley JS, Edwards JE, Gilbert D, Rice LB, Scheld M, Spellberg B, Bartlett J. Bad bugs, no drugs: no ESKAPE! An update from the Infectious Diseases Society of America. Clin. Infect. Dis. 2009; 48:1–12. [PubMed: 19035777]

(2). Chen W, Biswas T, Porter VR, Tsodikov OV, Garneau-Tsodikova S. Unusual regioversatility of acetyltransferase Eis, a cause of drug resistance in XDR-TB. Proc. Natl. Acad. Sci. U.S.A. 2011; 108:9804–9808. [PubMed: 21628583]

(3). Houghton JL, Biswas T, Chen W, Tsodikov OV, Garneau-Tsodikova S. Chemical and structural insights into the regioversatility of the aminoglycoside acetyltransferase Eis. ChemBioChem. 2013; 14:2127–2135. [PubMed: 24106131]

(4). Zaunbrecher MA, Sikes RD Jr. Metchock B, Shinnick TM, Posey JE. Overexpression of the chromosomally encoded aminoglycoside acetyltransferase eis confers kanamycin resistance in *Mycobacterium tuberculosis*. Proc. Natl. Acad. Sci. U.S.A. 2009; 106:20004–20009. [PubMed: 19906990]

(5). Georghiou SB, Magana M, Garfein RS, Catanzaro DG, Catanzaro A, Rodwell TC. Evaluation of genetic mutations associated with *Mycobacterium tuberculosis* resistance to amikacin, kanamycin and capreomycin: a systematic review. PLoS One. 2012; 7(No. e33275)

(6). Rodwell TC, Valafar F, Douglas J, Qian L, Garfein RS, Chawla A, Torres J, Zadorozhny V, Kim MS, Hoshide M, Catanzaro D, Jackson L, Lin G, Desmond E, Rodrigues C, Eisenach K, Victor TC, Ismail N, Crudu V, Gler MT, Catanzaro A. Predicting extensively drug-resistant *Mycobacterium tuberculosis* phenotypes with genetic mutations. J. Clin, Microbiol. 2014; 52:781–789. [PubMed: 24353002]

(7). Gikalo MB, Nosova EY, Krylova LY, Moroz AM. The role of eis mutations in the development of kanamycin resistance in *Mycobacterium tuberculosis* isolates from the Moscow region. J. Antimicrob. Chemother. 2012; 67:2107–2109. [PubMed: 22593564]

(8). Green KD, Chen W, Houghton JL, Fridman M, Garneau-Tsodikova S. Exploring the substrate promiscuity of drug-modifying enzymes for the chemoenzymatic generation of *N*-acylated aminoglycosides. ChemBioChem. 2010; 11:119–126. [PubMed: 19899089]

(9). Green KD, Chen W, Garneau-Tsodikova S. Effects of altering aminoglycoside structures on bacterial resistance enzyme activities. Antimicrob. Agents Chemother. 2011; 55:3207–3213. [PubMed: 21537023]

(10). Chen W, Green KD, Tsodikov OV, Garneau-Tsodikova S. Aminoglycoside multiacetylating activity of the enhanced intracellular survival protein from *Mycobacterium smegmatis* and its inhibition. Biochemistry. 2012; 51:4959–4967. [PubMed: 22646013]

(11). Pricer RE, Houghton JL, Green KD, Mayhoub AS, Garneau-Tsodikova S. Biochemical and structural analysis of aminoglycoside acetyltransferase Eis from *Anabaena variabilis*. Mol. BioSyst. 2012; 8:3305–3313. [PubMed: 23090428]

(12). Chen W, Green KD, Garneau-Tsodikova S. Cosubstrate tolerance of the aminoglycoside resistance enzyme Eis from *Mycobacterium tuberculosis*. Antimicrob. Agents Chemother. 2012; 56:5831–5838. [PubMed: 22948873]

(13). Dahl JL, Wei J, Moulder JW, Laal S, Friedman RL. Subcellular localization of the intracellular survival-enhancing Eis protein of *Mycobacterium tuberculosis*. Infect. Immun. 2001; 69:4295–4302. [PubMed: 11401966]

(14). Samuel LP, Song CH, Wei J, Roberts EA, Dahl JL, Barry CE 3rd, Jo EK, Friedman RL. Expression, production and release of the Eis protein by *Mycobacterium tuberculosis* during infection of macrophages and its effect on cytokine secretion. Microbiology. 2007; 153:529–540. [PubMed: 17259625]

(15). Lella RK, Sharma C. Eis (enhanced intracellular survival) protein of *Mycobacterium tuberculosis* disturbs the cross regulation of T-cells. J. Biol. Chem. 2007; 282:18671–18675. [PubMed: 17449476]

(16). Ganaie AA, Lella RK, Solanki R, Sharma C. Thermostable hexameric form of Eis (Rv2416c) protein of *M. tuberculosis* plays an important role for enhanced intracellular survival within macrophages. PLoS One. 2011; 6(No. e27590)

(17). Kim KH, An DR, Song J, Yoon JY, Kim HS, Yoon HJ, Im HN, Kim J, Kim do J, Lee SJ, Kim KH, Lee HM, Kim HJ, Jo EK, Lee JY, Suh SW. *Mycobacterium tuberculosis* Eis protein initiates suppression of host immune responses by acetylation of DUSP16/MKP-7. Proc. Natl. Acad. Sci. U.S.A. 2012; 109:7729–7734. [PubMed: 22547814]

(18). Yoon HJ, Kim KH, Yang JK, Suh SW, Kim H, Jang S. A docking study of enhanced intracellular survival protein from *Mycobacterium tuberculosis* with human DUSP16/MKP-7. J. Synchrotron Radiat. 2013; 20:929–932. [PubMed: 24121342]

(19). Green KD, Chen W, Garneau-Tsodikova S. Identification and characterization of inhibitors of the aminoglycoside resistance acetyltransferase Eis from *Mycobacterium tuberculosis*. ChemMedChem. 2012; 7:73–77. [PubMed: 21898832]

(20). Wei J, Dahl JL, Moulder JW, Roberts EA, O'Gaora P, Young DB, Friedman RL. Identification of a *Mycobacterium tuberculosis* gene that enhances mycobacterial survival in macrophages. J. Bacteriol. 2000; 182:377–384. [PubMed: 10629183]

(21). Esteban J, Ortiz-Perez A. Current treatment of atypical mycobacteriosis. Expert Opin. Pharmacother. 2009; 10:2787–2799. [PubMed: 19929702]

(22). Nessar R, Cambau E, Reyrat JM, Murray A, Gicquel B. *Mycobacterium abscessus*: a new antibiotic nightmare. J. Antimicrob. Chemother. 2012; 67:810–818. [PubMed: 22290346]

(23). Nessar R, Reyrat JM, Murray A, Gicquel B. Genetic analysis of new 16S rRNA mutations conferring aminoglycoside resistance in *Mycobacterium abscessus*. J. Antimicrob. Chemother. 2011; 66:1719–1724. [PubMed: 21652621]

(24). Cremades R, Santos A, Rodriguez JC, Garcia-Pachon E, Ruiz M, Royo G. *Mycobacterium abscessus* from respiratory isolates: activities of drug combinations. J. Infect. Chemother. 2009; 15:46–48. [PubMed: 19280301]

(25). Ho IIY, Chan CY, Cheng AFB. Aminoglycoside resistance in Mycobacterium kansasii, Mycobacterium avium-M. intracellulare, and *Mycobacterium fortuitum*: are aminoglycoside-modifying enzymes responsible? Antimicrob. Agents Chemother. 2000; 44:39–42. [PubMed: 10602720]

(26). Steinhaus EA. A study of the bacteria associated with thirty species of insects. J. Bacteriol. 1941; 42:757–790. [PubMed: 16560484]

(27). Lecomte J, St-Arnaud M, Hijri M. Isolation and identification of soil bacteria growing at the expense of arbuscular mycorrhizal fungi. FEMS Microbiol. Lett. 2011; 317:43–51. [PubMed: 21219415]

(28). Becker K, Rutsch F, Uekotter A, Kipp F, Konig J, Marquardt T, Peters G, von Eiff C. *Kocuria rhizophila* adds to the emerging spectrum of micrococcal species involved in human infections. J. Clin. Microbiol. 2008; 46:3537–3539. [PubMed: 18614658]

(29). Moissenet D, Becker K, Merens A, Ferroni A, Dubern B, Vu-Thien H. Persistent bloodstream infection with *Kocuria rhizophila* related to a damaged central catheter. J. Clin. Microbiol. 2012; 50:1495–1498. [PubMed: 22259211]

(30). Biswas T, Houghton JL, Garneau-Tsodikova S, Tsodikov OV. The structural basis for substrate versatility of chloramphenicol acetyltransferase CATI. Protein Sci. 2012; 21:520–530. [PubMed: 22294317]

(31). Houghton JL, Green KD, Pricer RE, Mayhoub AS, Garneau-Tsodikova S. Unexpected *N*-acetylation of capreomycin by mycobacterial Eis enzymes. J. Antimicrob. Chemother. 2013; 68:800–805. [PubMed: 23233486]

(32). Vetting MW, Park CH, Hegde SS, Jacoby GA, Hooper DC, Blanchard JS. Mechanistic and structural analysis of aminoglycoside *N*-acetyltransferase AAC(6′)-Ib and its bifunctional, fluoroquinolone-active AAC(6′)-Ib-cr variant. Biochemistry. 2008; 47:9825–9835. [PubMed: 18710261]

(33). Kim KH, An DR, Yoon HJ, Yang JK, Suh SW. Structure of *Mycobacterium smegmatis* Eis in complex with paromomycin. Acta Crystallogr., Sect. F: Struct. Biol. Commun. 2014; 70:1173–1179. [PubMed: 25195887]

(34). Tsodikov OV, Green KD, Garneau-Tsodikova S. A random sequential mechanism of aminoglycoside acetylation by *Mycobacterium tuberculosis* Eis protein. PLoS One. 2014; 9(No. e92370)

(35). Tiago I, Maranha A, Mendes V, Alarico S, Moynihan PJ, Clarke AJ, Macedo-Ribeiro S, Pereira PJ, Empadinhas N. Genome sequence of *Mycobacterium hassiacum* DSM 44199, a rare source of heat-stable mycobacterial proteins. J. Bacteriol. 2012; 194:7010–7011. [PubMed: 23209251]

(36). Jennings BC, Labby KJ, Green KD, Garneau-Tsodikova S. Redesign of substrate specificity and identification of the aminoglycoside binding residues of Eis from *Mycobacterium tuberculosis*. Biochemistry. 2013; 52:5125–5132. [PubMed: 23837529]

(37). Green KD, Biswas T, Chang C, Wu R, Chen C, Janes BK, Chalupska D, Gornicki P, Hanna PC, Tsodikov OV, Joachimiak A. Biochemical and structural analysis of an Eis family aminoglycoside acetyltransferase from Bacillus anthracis. Biochemistry. 2015; in press. doi: 10.1021/acs.biochem.5b00244

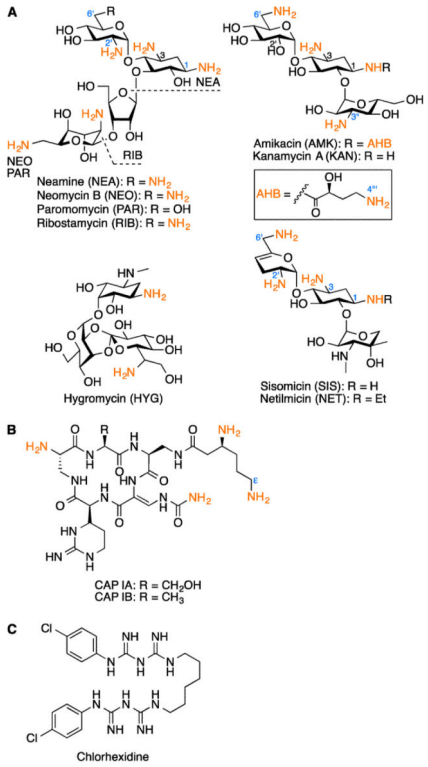

Figure 1.

Chemical structures of (A) all AGs found to be modified by Eis homologues in this study, (B) the polypeptide capreomycin (sold as a mixture of CAP IA and CAP IB), and (C) an Eis_*Mtb* inhibitor, chlorhexidine.

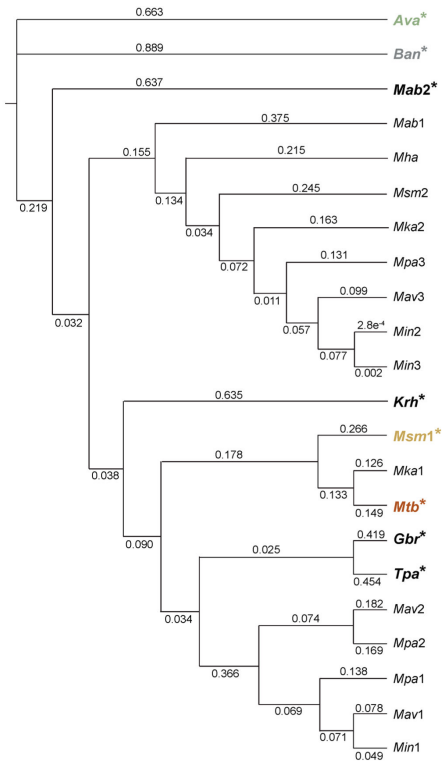

Figure 2.

Phylogenetic tree analysis of the 22 Eis homologues studied based on their amino acid sequences. The numbers are proportional to the distance of the evolutionary branches of the tree. The abbreviated names of the tree correspond to the following species and gene: *Anabaena variabilis* ATCC 29413 (*Ava*); *Bacillus anthracis* 34F2 Sterne strain (*Ban*); *Gordonia bronchialis* ATCC 25592 (*Gbr*); *Kocuria rhizophila* ATCC 9341 (*Krh*); *Mycobacterium abscessus* ATCC 19977 genes MAB4124 (*Mab*1) and MAB4532c (*Mab*2); *Mycobacterium avium* subsp. *avium* ATCC 25291 genes MaviaA2_07418 (*Mav*1), MaviaA2_15865 (*Mav*2), and MaviaA2_00691 (*Mav*3); *Mycobacterium hassiacum* DSM 44199 (*Mha*); *Mycobacterium intracellulare* ATCC 13950 genes MintA_24600 (*Min*1), MintA_21739 (*Min*2), and OCU_01560 (*Min*3); *Mycobacterium kansassii* ATCC 12478 genes *Mka*n A1_16037 (*Mka*1) and *Mka*n A1_05800 (*Mka*2); *Mycobacterium parascrofulaceum* ATCC BAA-614 genes ZP_06852004 (*Mpa*1), ZP_06848356 (*Mpa*2), and ZP_06849426 (*Mpa*3); *Mycobacterium smegmatis* MC2 155 genes MSMEG_3513 (*Msm*1) and MSMEG_4540 (*Msm*2); *Mycobacterium tuberculosis* H37Rv (*Mtb*); *Tsukamurella paurometabola* ATCC 8368 (*Tpa*). Active enzymes are indicated with an asterisk. The percent identity of each homologue compared to that of Eis_*Mtb* is presented in the Supporting Information (Table S1).

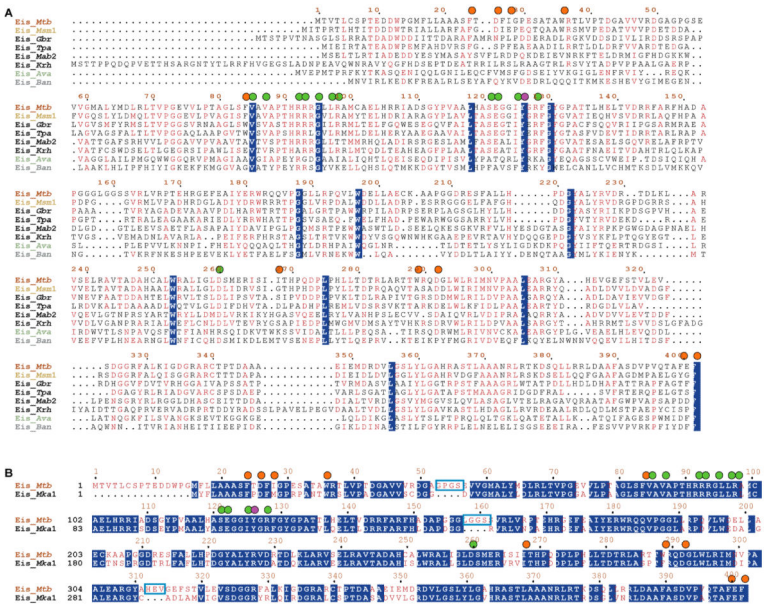

Figure 3.

(A) Alignment of all Eis homologue protein sequences found to be active in acetylating AGs in this work. (B) Alignment of Eis_*Mtb* and its closest homologue in amino acid sequence tested, Eis_*Mka*1. Turquoise boxes indicate areas of difference for the *Mka*1 homologue, which are hypothesized to be important in protein–protein interactions of the Eis monomers. For both alignments, the catalytic tyrosine (Y) residue is indicated with a purple circle, AG-binding site residues are indicated with orange circles, and AcCoA-binding site residues are indicated with green circles. All of the residues marked with colored circles were originally identified by site-directed mutagenesis of the Eis_*Mtb* enzyme.[2,36] White letters with blue background indicate amino acids completely conserved throughout the sequences, whereas red residues indicate amino acids highly conserved throughout the sequences.

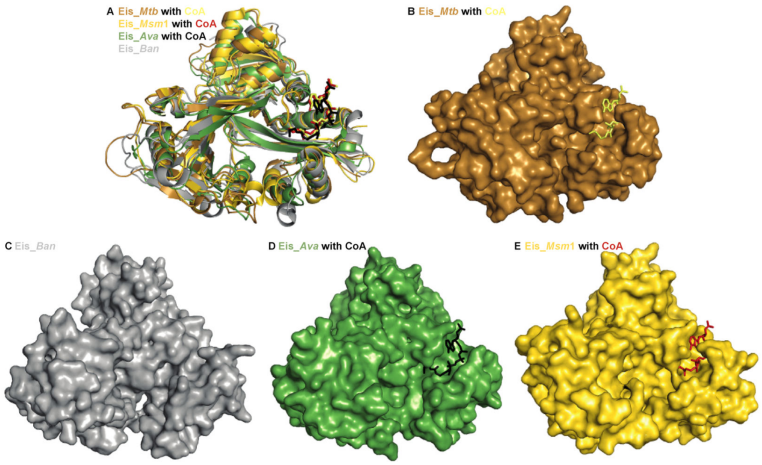

Figure 4.

Comparison of crystal structures of Eis_*Mtb* (PDB 3R1K, 1.95 Å),[2] Eis_*Msm*1 (PDB 3SXN, 2.03 Å),[17] Eis_*Ava* (PDB 2OZG, 2.00 Å),[11] and Eis_*Ban* (PDB 3N7Z, 2.75 Å). (Only one monomer of these hexameric structures is shown for clarity.) Panel A depicts the overlay of one monomer from each of the four structures and shows that there is little variation in the overall structure of this family of enzymes. Surface cartoons shown in panels B–E demonstrate subtle differences in the active sites of the Eis homologues from (B) *Mycobacterium tuberculosis* (shown in brown with CoA as yellow stick), (C) *Bacillus anthracis* (shown in gray in the absence of CoA), (D) *Anabaena variabilis* (shown in green with CoA as black stick), and (E) *Mycobacterium smegmatis* (shown in gold with CoA as red stick).

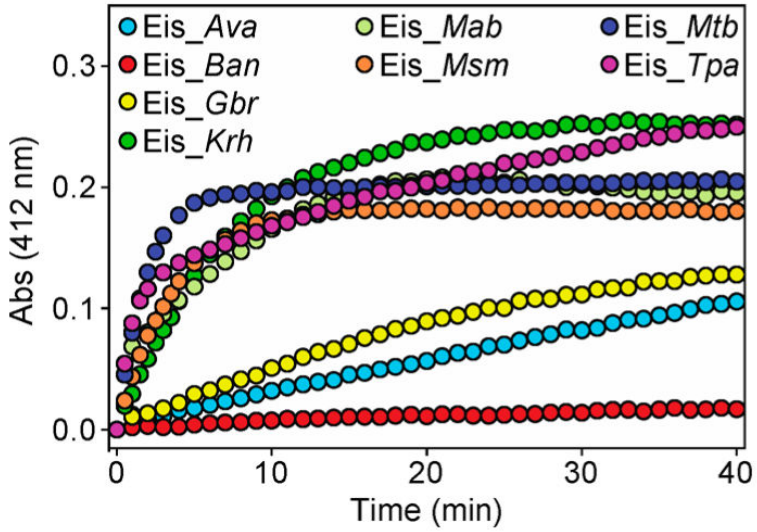

Figure 5.
UV–vis curves monitoring the acetylation of CAP by various Eis homologues.

Table 1

Comparison of the Number of Modifications for Reactions of Eis Homologues with Various AGs and AcCoA or ProCoA[a]

				AcCoA				
AG	Eis_*Ava*[b]	Eis_*Ban*[c]	Eis_*Gbr*	Eis_*Krh*	Eis_*Mab*	Eis_*Msm*1[b,d]	Eis_*Mtb*[b,c,d,e]	Eis_*Tpa*
AMK	tri	di	di	di	×	tri	tri	tri
HYG	×	di	mono	mono	mono	mono	di	di
KAN	mono	di	mono	di	di	di	di	di
NEA	tri	tri	tri	tri	tri	tri	tri	tri
NEO	tri	tri	tri	tetra	tetra	tri	tri	tetra
NET	di	mono	mono	di	di	di	di	di
PAR	tri	tri	tri	tri	tri	tri	di	tri
RIB	tri	tri	di	di	di	tri	tri	di
SIS	di	di	di	tri	di	tri	tri	di
				ProCoA				
AG	Eis_*Ava*	Eis_*Ban*	Eis_*Gbr*	Eis_*Krh*	Eis_*Mab*	Eis_*Msm*1	Eis_*Mtb*[e]	Eis_*Tpa*
AMK	mono	di	di	mono	×	di	di	di
HYG	×	di	mono	mono	mono	mono	mono	mono
KAN	mono	mono	mono	mono	di	di	di	di
NEA	di	tri	di	di	tri	di	di	tri
NEO	di	tri	tri	di	di	tri	tri	di
NET	mono	mono	mono	mono	di	mono	mono	di
PAR	di	di	di	di	tri	di	mono	tri
RIB	di	tri	di	di	di	di	di	di
SIS	di	di	di	di	di	mono	mono	di

[a] × indicates that the AG is not a substrate for the enzyme tested.

[b] Data from ref 11.

[c] Data from ref 37.

[d] Data from ref 10.

[e] Data from ref 12.

Table 2

Kinetic Parameters Determined for Eis Homologues from Various Species by Using AcCoA with different AGs

Eis homologue	AG	K_m (μM)	k_{cat} (s^{-1})	k_{cat}/K_m (M^{-1} s^{-1})	$k_{cat}Xxx/k_{cat}Mtb$	$k_{cat}/K_mXxx/k_{cat}/K_mMtb$
Eis_*Ava*[a]	KAN	1002 ± 43	0.205 ± 0.004	205 ± 9	0.39	0.13
	PAR	237 ± 36	0.183 ± 0.013	773 ± 132	1.35	0.48
Eis_*Ban*[b]	KAN	57 ± 9	0.135 ± 0.008	2368 ± 399	0.26	1.49
	PAR	44 ± 11	0.019 ± 0.001	432 ± 110	0.14	0.35
Eis_*Gbr*	KAN	1020 ± 350	0.672 ± 0.036	659 ± 229	1.28	0.41
	PAR	763 ± 150	2.05 ± 0.18	2687 ± 579	15.07	2.17
Eis_*Krh*	KAN	268 ± 47	0.042 ± 0.002	157 ± 28	0.08	0.10
	PAR	435 ± 52	1.68 ± 0.07	3862 ± 406	12.35	3.12
Eis_*Mab*2	KAN	125 ± 27	0.124 ± 0.007	992 ± 377	0.24	0.62
	PAR	144 ± 14	2.83 ± 0.07	19653 ± 1972	20.80	15.90
Eis_*Msm*1[a,c]	KAN	665 ± 42	0.360 ± 0.010	541 ± 37	0.68	0.34
	PAR	738 ± 158	0.235 ± 0.033	318 ± 82	1.73	0.26
Eis_*Mtb*[a,c]	KAN	330 ± 40	0.526 ± 0.027	1594 ± 250	1.00	1.00
	PAR	110 ± 21	0.136 ± 0.012	1236 ± 260	1.00	1.00
Eis_*Tpa*	KAN	35 ± 8	0.163 ± 0.007	4657 ± 1083	0.31	2.92
	PAR	180 ± 10	5.92 ± 0.09	32889 ± 1894	43.53	26.60

[a]Data from ref 11.

[b]Data from ref 37.

[c]Data from ref 36.

Table 3

Comparison of the Cosubstrate Tolerance for Eis Homologues from Various Species Using NEO as the Substrate[a]

acyl-CoA	Eis_*Ava*[b]	Eis_*Ban*	Eis_*Gbr*	Eis_*Krh*	Eis_*Mab*	Eis_*Msm*1	Eis_*Mtb*[c]	Eis_*Tpa*
Ac	√	√	√	√	√	√	√	√
Pro	√	√	√	√	√	√	√	√
n-butanoyl	×	×	×	×	×	×	×	×
n-hexanoyl	×	×	×	×	×	×	×	×
octanoyl	×	×	×	×	×	×	×	×
decanoyl	×	×	×	×	×	×	×	×
lauroyl	×	×	×	×	×	×	×	×
myristoyl	×	×	×	×	×	×	×	×
palmitoyl	×	×	×	×	×	×	×	×
crotonyl	×	×	×	×	×	×	√	×
malonyl	×	×	×	√	×	×	√	×
i-valeryl	×	×	×	×	×	×	×	×

[a] × indicates that the acyl-CoA is not a cosubstrate of the Eis enzyme tested; √ indicates that the acyl-CoA is a cosubstrate of the Eis enzyme tested.

[b] Data from ref 11.

[c] Data from ref 12.

Table 4

Sequential Reactions Using ProCoA Followed by AcCoA and Competition Assays in Which Reactions Were Performed with both AcCoA and ProCoA[a]

	ProCoA → AcCoA[b]							
AG	Eis_*Ava*	Eis_*Ban*	Eis_*Gbr*	Eis_*Krh*	Eis_*Mab*	Eis_*Msm*1	Eis_*Mtb*[c]	Eis_*Tpa*
AMK	mono-Ac	ND	ND	mono-Ac-mono-Pro	×	mono-Ac-mono-Pro	mono-Ac-di-Pro	di-Pro
	mono-Pro					di-Pro		mono-Ac-di-Pro
						mono-Ac-di-Pro		
HYG	×	ND	ND	ND	ND	ND	mono-Pro	mono-Pro
								mono-Ac-mono-Pro
KAN	ND	mono-Pro	ND	di-Ac	ND	ND	di-Pro	ND
				mono-Ac-mono-Pro				
NEA	di-Pro	ND	mono-Pro	mono-Ac-mono-Pro	ND	mono-Ac-Mono-Pro	mono-Ac-di-Pro	ND
			mono-Ac-mono-Pro			di-Pro		
			di-Pro			di-Ac-mono-Pro		
			di-Ac-mono-Pro			mono-Ac-di-Pro		
			mono-Ac-di-Pro					
NEO	di-Ac	ND	ND	mono-Ac-di-Pro	mono-Ac-di-Pro	ND	tri-Pro	di-Ac-Pro
	mono-Ac-mono-Pro							mono-Ac-di-Pro
	mono-Ac-di-Pro							tri-Ac-Pro
								di-Ac-di-Pro
NET	ND	ND	ND	mono-Ac	ND	mono-Pro	mono-Pro	ND
				mono-Pro				
				di-Ac				
				mono-Ac-mono-Pro				
PAR	mono-Ac-mono-Pro	di-Pro	mono-Ac-di-Pro	mono-Ac-di-Pro	ND	mono-Ac-mono-Pro	mono-Ac-mono-Pro	ND
	di-Pro					di-Pro		
						di-Ac-mono-Pro		
						mono-Ac-di-Pro		
RIB	mono-Pro	ND	ND	ND	ND	di-Pro	di-Pro	ND
	di-Ac							
	mono-Ac-mono-Pro							
	di-Pro							
	mono-Ac-di-Pro							
SIS	ND	ND	ND	mono-Pro	ND	mono-Pro	mono-Pro	ND

				mono-Ac-mono-Pro di-Pro				
				AcCoA + ProCoA[d]				
AG	Eis_*Ava*	Eis_*Ban*	Eis_*Gbr*	Eis_*Krh*	Eis_*Mab*	Mab_*Msm*1	Eis_*Mtb*[c]	Eis_*Tpa*
AMK	mono-Ac	di-Ac	mono-Ac	mono-Ac	×	di-Ac	di-Ac	di-Ac
	di-Ac		mono-Ac-mono-Pro	di-Ac			tri-Ac	
	mono-Ac-mono-Pro			mono-Ac-mono-Pro				
HYG	×	mono-Ac	mono-Ac	mono-Ac	mono-Ac	mono-Ac	mono-Ac	mono-Ac
		di-Ac					mono-Ac-mono-Pro	di-Ac
KAN	mono-Ac	mono-Ac	mono-Ac	di-Ac	di-Ac	di-Ac	di-Ac	di-Ac
			mono-Pro					
NEA	mono-Ac	di-Ac	mono-Ac	di-Ac	tri-Ac	di-Ac	tri-Ac	di-Ac
	mono-Pro	tri-Ac	mono-Pro		di-Ac-mono-Pro		di-Ac-mono-Pro	tri-Ac
	di-Ac	di-Ac-mono-Pro						
	tri-Ac	mono-Ac-di-Pro						
NEO	mono-Ac	di-Ac	di-Ac	di-Ac	tri-Ac	tri-Ac	tri-Ac	mono-Ac
	di-Ac	mono-Ac-mono-Pro	di-Pro	mono-Ac-mono-Pro	di-Ac-mono-Pro		tri-Pro	mono-Pro
	mono-Ac-mono-Pro	di-Pro	tri-Ac		tetra-Ac			di-Ac
		mono-Ac-di-Pro	di-Ac-mono-Pro		tri-Ac-mono-Pro			mono-Ac-mono-Pro
			mono-Ac-di-Pro		di-Ac-di-Pro			tri-Ac
			tri-Pro					
NET	mono-Ac	mono-Ac	mono-Ac	mono-Ac	mono-Ac	mono-Ac	mono-Ac	mono-Ac
	mono-Pro	mono-Pro	mono-Pro		di-Ac		di-Ac	di-Ac
	mono-Ac-mono-Pro				mono-Ac-mono-Pro			mono-Ac-mono-Pro
					di-Pro			
PAR	di-Ac	di-Ac	di-Ac	di-Ac	tri-Ac	di-Ac	di-Ac	di-Ac
	tri-Ac	mono-Ac-di-Pro	mono-Ac-mono-Pro					tri-Ac
RIB	di-Ac	mono-Ac	mono-Ac	di-Ac	di-Ac	mono-Ac	di-Ac	di-Ac
	mono-Ac-mono-Pro	mono-Pro	mono-Pro			di-Ac		
		di-Ac	di-Ac					
SIS	mono-Ac	mono-Ac	mono-Ac	mono-Ac	di-Ac	mono-Pro	mono-Ac	di-Ac
	di-Ac	di-Ac	di-Ac	di-Ac			di-Ac	
	mono-Ac-mono-Pro	mono-Ac-mono-Pro		mono-Ac-mono-Pro			mono-Ac-mono-Pro	

[a] × indicates that the reaction was not tested as the AG was found to not be a substrate of the enzyme; ND indicates that the reaction was not tested because the number of *n*-propionylations was equal to the number of acetylations.

[b] Reactions with ProCoA were followed by incubation with AcCoA.

[c] Data from ref 12.

[d] AcCoA and ProCoA were incubated with Eis and AG in a 1:1 ratio.

Table 5

IC_{50} Values of the Known Eis_*Mtb* Inhibitor Chlorhexidine with Eis Homologues

Eis species	chlorhexidine (μM)	IC_{50}*Xxx*/IC_{50}*Mtb*
Ava	20 ± 7[a]	111
Ban	14 ± 4[b]	77
Gbr	4.4 ± 0.6	23
Krh	17 ± 4	91
Mab	4.4 ± 0.9	23
*Msm*1	1.9 ± 0.4[a]	10
Mtb	0.188 ± 0.030[c]	1
Tpa	7.4 ± 1.6	40

[a]Data from ref 11.

[b]Data from ref 37.

[c]Data from ref 19.